III.D.4 Determination of Electrochemical Performance and Thermo-Mechanical-Chemical Stability of SOFCs from Defect Modeling

Eric D. Wachsman (Primary Contact), Keith L. Duncan, Fereshteh Ebrahimi
Department of Materials Science and Engineering
University of Florida
Gainesville, Florida 32611
Phone: (352) 846-2991; Fax: (352) 392-3771; E-mail: ewach@mse.ufl.edu

DOE Project Manager: Travis Shultz
Phone: (304) 285-1370; E-mail: Travis.Shultz@netl.doe.gov

Objectives

- Advance the fundamental understanding of the continuum-level electrochemistry of oxide mixed ionic-electronic conductors in relation to their performance in solid oxide fuel cells (SOFCs).
- Obtain, from experiments, fundamental constants required for implementing the continuum-level electrochemical model.
- Extend the models to multi-layer structures and incorporate microstructural effects.
- Verify the models through experiments.
- Develop a transient version of the continuum-level electrochemical model.
- Obtain time constants for various transport processes from electrical impedance spectroscopy to examine the effects of transients on SOFC performance.
- Develop and deliver software modules for incorporation of the continuum-level electrochemical model into SOFC failure analysis software used by the National Energy Technology Laboratory (NETL), Pacific Northwest National Laboratory (PNNL), Oak Ridge National Laboratory (ORNL) and the Solid State Energy Conversion Alliance (SECA) industrial teams.

Approach

- Develop a continuum-level electrochemical model for the generation, distribution and transport of defects in oxide mixed ionic-electronic conductors (MIECs).
- Extend model to thermo-mechanical properties, thermochemical stability and transient behavior of oxide MIECs.
- Extend model to multi-layer (anode-electrolyte-cathode) SOFCs.
- Incorporate microstructural effects into the continuum-level electrochemical model.
- Design and conduct experiments to explore the thermo-mechanical, thermochemical and transient behavior of oxide MIECs and verify the continuum-level electrochemical model.
- Analyze experimental results and interpret them in framework of model.
- Feed back experimental results into model and validate it.

Accomplishments

- Completed the continuum-level electrochemical model for *steady-state* conditions, using potential dependent boundary conditions and non-linear Galvani potential.
- Completed the continuum-level electrochemical model for *transient* conditions, using potential dependent boundary conditions and a linear Galvani potential.

- Compiled software modules for vacancy concentration and electron concentration in *n*-type and *p*-type mixed ionic-electronic conductors.
- Extended the continuum-level electrochemical model to thermo-mechanical and thermochemical properties of mixed ionic-electronic conductors.
- Extended the continuum-level electrochemical model to yttria-stabilized zirconia (YSZ)/lanthanum strontium manganate (LSM) bilayer.
- Measured the thermal expansion of ceria and samaria-doped ceria in air and reducing atmospheres.
- Measured the elastic moduli of pure ceria and gadolinia-doped ceria in reducing (H_2) and oxidizing (air) atmospheres using nondestructive and (nanoscale) destructive techniques; both showed that reducing conditions cause a ~30% decrease in the elastic modulus relative to air.

Future Directions

- Complete the extension of the continuum-level electrochemical model to multi-layer SOFC architecture.
- Incorporate microstructural effects into the continuum-level electrochemical model.
- Minimize uncertainty in the deconvolution of electrical impedance spectra for more accurate assessment of time constants for electrochemical processes.
- Obtain more data points for the elastic moduli of ceria, gadolinia-doped ceria and YSZ within the range of oxygen partial pressures (Po_2) between air and H_2/H_2O using both nondestructive and (nanoscale) destructive techniques.
- Obtain data for the thermo-mechanical properties of polycrystalline YSZ as a function of Po_2 between air and H_2/H_2O.
- Obtain thermal expansion data for Ni-YSZ, LSM, YSZ and other MIECS in various (reducing or oxidizing) atmospheres.
- Experimentally determine effect of microstructure on transient behavior of SOFCs.

Introduction

SOFCs are the future of energy production. They offer great promise as a clean and efficient process for directly converting chemical energy from a fuel to electricity while providing significant environmental benefits (they produce negligible hydrocarbons, CO, or NO_x and, as a result of their high efficiency, produce about one-third less CO_2 per kilowatt hour than internal combustion engines). Moreover, SOFCs are fuel flexible, expanding the range of fuels that can be used in the conversion process from conventional fuels to hydrogen.

For extensive deployment of SOFCs into industrial and consumer markets to become a reality, some key hurdles need to be cleared. Three of these hurdles are the (i) thermo-mechanical, (ii) thermochemical and (iii) transient stability of SOFCs. In our research, we are tackling these hurdles by developing models to relate point defect (atomic-scale anomalies) population distribution and microstructure (the fine structure of a material) to the electrochemical and mechanical properties of SOFC components, which are then the actual determinants of the thermo-mechanical, thermochemical and transient stability of SOFCs. These fundamental-level models can then be incorporated into system-level models to predict and analyze SOFC performance and response (transient and steady-state) to various inputs.

Approach

To develop models relating point defect population distribution and microstructure to the electrochemical and mechanical properties of SOFC components, first we modeled the generation of point defects in oxide MIECs as a function of atmosphere (Po_2) and temperature. Since SOFCs operate in a Po_2 gradient, next we modeled the transport and distribution of defects in an MIEC in a Po_2 gradient by solving the Nernst-Planck, mass conservation and charge conservation equations for Laplacian and

non-Laplacian potential distributions. These two steps produced a continuum-level electrochemical model that relates point defect concentration to operating conditions (such as temperature, Po_2 gradient and load voltage) and material properties (such as the mass action constant for oxygen exchange between the oxide and the ambient, and ionic and electronic diffusivity). Hence, by modeling or applying relationships between point defects and indices for thermo-mechanical, thermochemical and transient stability, secondary relationships between these indices and the SOFC operating conditions and material properties can be derived.

An essential complement to the models developed in our research is experimental verification. To this end, experiments are being conducted to confirm the predictions of the models as well as to give more insight into the factors and mechanisms that play a role in the performance of the SOFC components and the overall stability of the SOFC.

Results

Continuum-Level Electrochemical Model-Defect Thermodynamics. To obtain defect concentration dependence on Po_2 requires the solution of a system of equations consisting of mass action equations from the defect equilibria and charge, mass and site balance equations. However, depending on the defect species involved, the system of equations can result in high order (>3) polynomials with no analytical solution. The traditional way of simplifying such equation systems is the Brouwer method, which divides the equilibria into separate Brouwer regimes where two species dominate [1]. This method generates defect concentration dependence on Po_2 in each Brouwer regime. However, it produces formulae that are discontinuous across the Brouwer regimes. This is a problem for some MIECs in a Po_2 gradient where the defect equilibria span more than one regime. Moreover, an electrical potential can drive an MIEC from one regime to the next. Conversely, by considering three defects instead of two, we have derived equations that are continuous across all regimes. Examples of these, for oxide MIECs, follow:

$$c_V(P_{O_2}) = \left[\tfrac{3}{4}K_r^{\frac{1}{2}}P_{O_2}^{-\frac{1}{4}} + \left(\tfrac{1}{2}c_A\right)^{\frac{3}{2}}\right]^{\frac{2}{3}}$$

and

$$c_e(P_{O_2}) = K_r^{\frac{1}{2}}P_{O_2}^{-\frac{1}{4}}\left[\tfrac{3}{4}K_r^{\frac{1}{2}}P_{O_2}^{-\frac{1}{4}} + \left(\tfrac{1}{2}c_A\right)^{\frac{3}{2}}\right]^{\frac{1}{3}} \quad (1)$$

where c_V, c_e and c_A are the concentrations of vacancies, electrons and a trivalent acceptor dopant, respectively. K_r is the equilibrium constant for the oxygen exchange between the oxide and gaseous O_2. The full derivation may be found in our earlier work [2]. Equation (1) is a low Po_2 simplification of more general equations we developed for fluorites and perovskites [2]. Finally, excellent results were obtained when these equations were fitted to experimental data [3] with K_r as the sole fitting parameter.

Continuum-Level Electrochemical Model-Defect Transport. To model defect transport in MIECs, we solved the Nernst-Planck, material balance, and current density equations [4]. To simplify the equations and make the derivations more tractable, previous researchers have assumed a linear, i.e., Laplacian, potential distribution. We have been able to relax that assumption and solve for the more general Poisson potential distribution where the Galvani potential is not forced to vary linearly with position inside the MIEC.

In steady-state conditions, the solutions for oxygen vacancy concentration as a function of distance (x), for *n*-type oxide MIECs, are as follows [2, 5]:

$$c_V(x) - c_{V_0} - \frac{(D_V\gamma - j_V)c_A}{z_V(z_V - z_e)D_V\gamma}\cdot\ln\frac{z_V(z_V - z_e)D_V\gamma c_V(x) - j_V c_A}{z_V(z_V - z_e)D_V\gamma c_{V_0} - j_V c_A} = -\gamma x \quad (2)$$

where z is charge equivalence, q is the elementary electronic charge, j is flux density, Φ is Galvani potential, u is electrical mobility, L is MIEC thickness and $\gamma = (\Delta\phi/\lambda - Cv_L + Cv_0)/L$. The subscripts 0 and L refer to the boundary values of the MIEC, i.e., at x = 0 (anode side) and x = L (cathode side). Also, from the local equilibrium approximation,

$\Delta\phi = \Phi_{ext} - \Phi_{th} - k_BT(z_vq)^{-1}\ln(Cv_L/Cv_0)$,

and from the equivalent circuit of an SOFC,

$$\bar{t}_{ion}\Phi_{th} = \eta + \Phi_{ext}$$

where $\bar{t}_{ion}$ is average transference number, Φ_{ext} is load voltage, Φ_{th} is the Nernst potential and η is cell overpotential [6].

Previous researchers [6-8] used fixed boundary values for the defect concentrations and linear potential distributions. *Fixed* boundary values are independent of the load voltage, Φ_{ext}. This implies that Φ_{ext} only affects the spatial distribution of defects inside the MIEC. In principle, this is not possible, since the activities of all the reacting chemical species cannot be held constant while changing the potential at the interface [4, 9]. Potential-dependent boundary conditions were obtained by including the effect of the load voltage on the boundary values of the defect concentrations [5]. Our results, exemplified in Equation (2), allow for the prediction of the transport properties of the MIEC components and SOFC performance. As an example, we will consider the current and power efficiency of an SOFC, which are given by $\zeta_J = J/J_V$ and $\zeta_P = \zeta_J\Phi_{ext}/\Phi_{th}$, respectively, where J is current density.

Figure 1 shows a comparison of current and power efficiencies calculated from models with different assumptions for a doped ceria electrolyte. The figure shows that using fixed boundary conditions and assuming a linear Galvani potential leads to an overestimation of both current and power efficiencies. Assuming a linear potential ignores the efficiency-sapping effects of mixed conduction, and using *fixed* (i.e., independent of potential) boundary concentrations reduces the effects of changing concentration gradients. Consequently, when these assumptions are removed, the calculated efficiencies are smaller. These results emphasize the importance of using the correct electrochemical model as the basis for computation of relevant properties.

Thermo-Mechanical Properties. We now seek to extend the model developed above to the thermo-mechanical properties of MIECs. The relationship between defect population and elastic modulus-which is related to another crucial property: fracture toughness-may be derived by considering that the bond energy, E, between atoms in a crystal may be

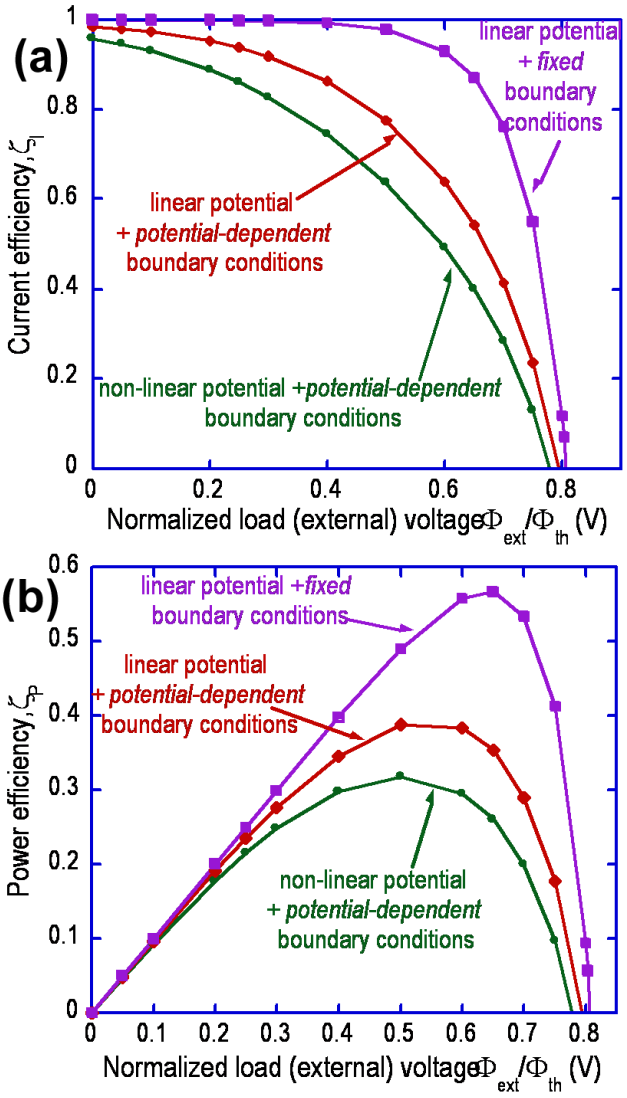

Figure 1. Comparison of current and power efficiency from various models for an SOFC.

approximated by $E = A/r^n - B/r^m$ [10], where r is the inter-atomic distance, and A, B, n and m are empirically determined constants ($m < n$). Thus, the elastic modulus for a perfect crystal, Y, may be approximated by: $1/r_0(\mathrm{d}^2E/\mathrm{d}r^2)_{r=r^0}$. In addition, the lattice constant, a, is proportional to r_0 (the average inter-atomic separation), and a has been shown to increase linearly with c_V [11, 12]. Thus, Y becomes

$$Y(x) \approx Y^*\left(\theta c_V(x) + 1\right)^{-(m+3)} \quad (3)$$

where Θ is an empirically determined constant, and the superscript "*" refers to stoichiometric

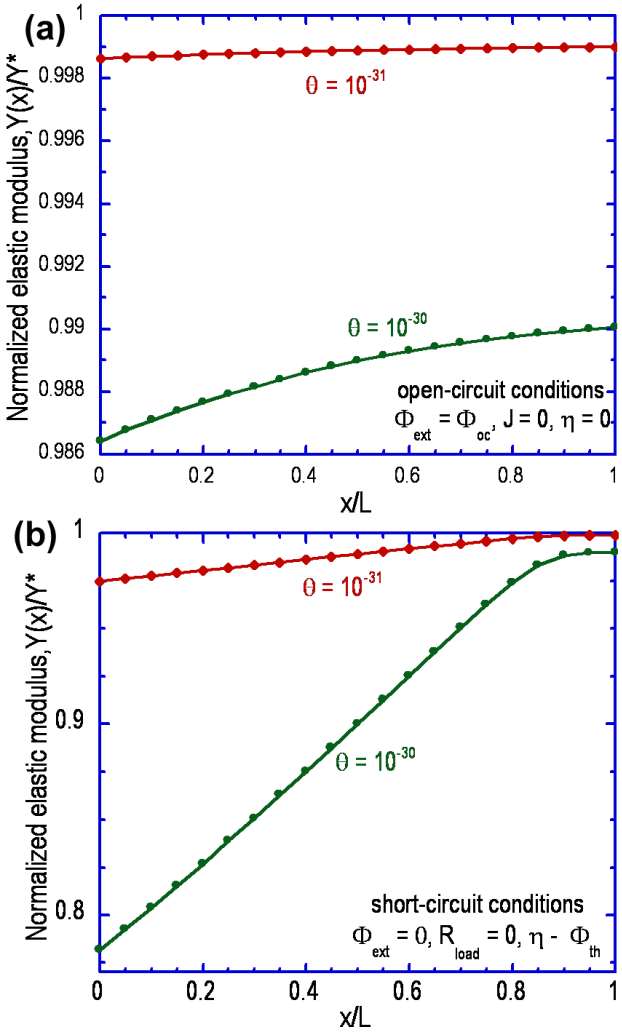

Figure 2. Elastic modulus profiles in (a) open-circuit and (b) short-circuit for samaria-doped ceria electrolyte, at 800 °C; anode is at $x = 0$ (Po_2 = 10^{-20} atm), cathode at $x = L$ ($Po_2 = 0.21$ atm)

conditions-i.e., when $c_V = 0$. Similar expressions were also derived for fracture toughness.

Figure 2 shows the results of extending the continuum-level electrochemical model to mechanical properties such as the elastic modulus, Y, in this example. The plots show a general degradation of the elastic modulus towards the anode side ($x = 0$) of the electrolyte. Moreover, it is seen that the variation in the elastic modulus is much less in open-circuit conditions (smallest concentration gradients) than in short-circuit conditions (steepest concentration gradients) [6]. Thus, one may expect that the electrolyte gets *weaker* as more current passes through the cell.

Using a Hysitron® Triboindenter, we have measured the elastic modulus of individual grains of pure ceria samples annealed in an H_2 atmosphere. Our results, Table 1, show that annealing in H_2 causes a ~30 % reduction in the elastic modulus of the samples. Also, the low standard deviation in our results indicates isotropy of the elastic modulus. These results were independently confirmed by our collaborators at ORNL, who obtained similar results using an acoustic resonance analyzer. Clearly, the continuum-level electrochemical model can facilitate the prediction of the thermo-mechanical properties of SOFCs.

Table 1. Elastic Modulus of Ceria before and after Hydrogen Anneal

		Modulus, Y, (GPa)	Hardness, H (GPa)
On the surface	As sintered	220.22±7.08	9.52±1.15
	H_2 reduced	148.87±14.86	8.80±1.41
	Reduction (%)	**32.40**	**7.56**
At the center	As sintered	187.46±5.81	8.47±0.6905
	H_2 reduced	129.77±13.04	7.31±1.43
	Reduction (%)	**30.77**	**13.70**

In the near future, we will perform 3-point bend tests with a MTS instrument to obtain elastic modulus and fracture toughness data for polycrystalline samples. Fractured samples will also be examined with scanning electron microscopy and transmission electron microscopy to determine the sources of fracture.

Chemical Stability. The continuum-level electrochemical model has also been applied to the chemical stability of interfaces, e.g., YSZ/LSM. Not surprisingly, our early results indicate that for relevant insight into the stability of electrolyte-electrode interfaces, we will need to incorporate the microstructure of the electrode. We are in the process of doing just that.

Transient Response. The continuum-level electrochemical model has been extended to transient conditions (more detail may be obtained from the Phase 1 topical report of this project). To obtain solutions, we assumed a linear potential distribution. This assumption is best applied to predominantly

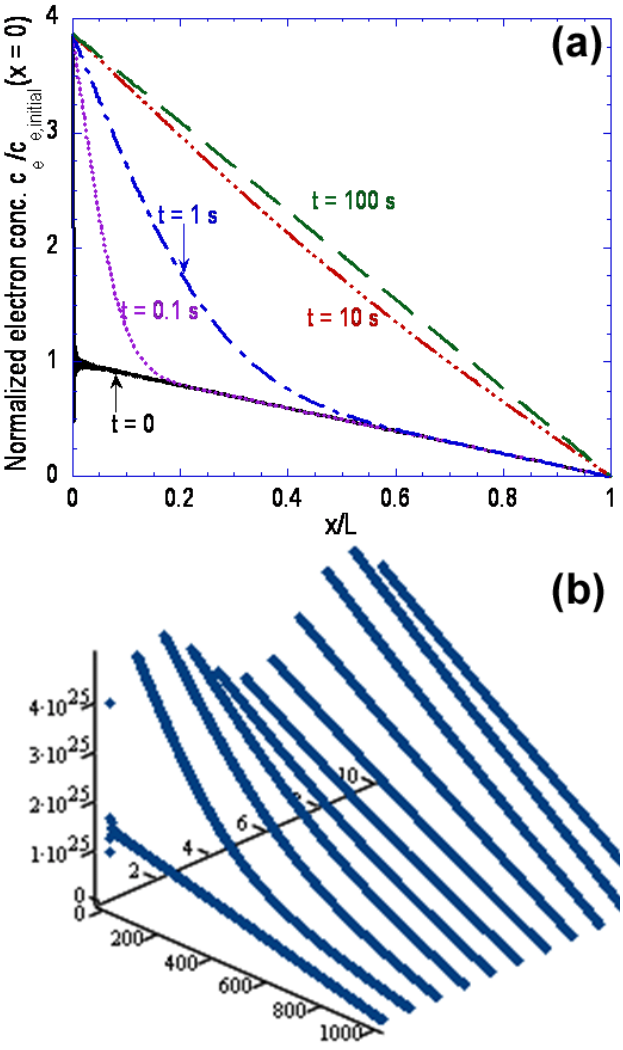

Figure 3. Time-dependent evolution of electron concentration profiles in a 1 mm thick YSZ electrolyte at 800 °C: (a) load voltage, Φ_{ext} goes from open-circuit value to $\Phi_{th}/4$ (b) Φ_{ext} has a 60 Hz sinusoidal *ripple*; anode is at x = 0 (Po_2 = 10^{-22} atm), cathode at x = 0 (Po_2 = 0.21 atm).

ionic conductors, e.g., YSZ, or predominantly electronic conductors, e.g., LSM.

Figure 3 shows the evolution of the electron concentration profiles in a 1 mm thick YSZ electrolyte. In Figure 3a a load (of voltage $\Phi_{th}/4$) is introduced to the SOFC, which was initially (at time, t = 0) in *open-circuit* conditions. The results show that while the boundary concentrations are established *instantly*, the concentration in the bulk lags behind, ostensibly limited by electron diffusivity and electrolyte thickness.

Figure 3b is a surface plot showing the spatial and temporal distribution of electron concentration, $c_e(x, t)$. In Figure 3b a load is again introduced to the SOFC, but this time it carries a 60-Hz sinusoidal *ripple* with it. The effect and presence of the *ripple* is evident in the plot, which shows an initial response similar to Figure 3a. However, after about 6 s, the lag is no longer evident even though the *ripple* persists. This is a result of the amplitude and frequency of the *ripple*. The amplitude is small enough not to cause great changes in the concentration gradient. The time constant of the electrolyte (~4.5 s) is ~ 270 times the period of the *ripple*. Hence, the electrolyte does not have enough time to respond to the *ripple* in the bulk, and the *ripple's* effect is seen only at the boundaries.

For transient defect transport, the total thickness of the MIEC, *L*, is a component of the time constant for the process such that the transient response of the MIEC depends exponentially on the electrolyte thickness. As the thickness of the electrolyte is reduced to 10 μm, the time scale decreases to ~0.05 s (approaching 60 Hz). This provides important criteria (impact of improved performance with thinner electrolytes versus susceptibility to higher transient voltages or fuel composition variations) if the SOFC is going to be used under transient conditions.

The challenge of accurately deconvoluting the significant transport mechanisms for electrical impedance spectra is proving to be formidable. Hence, we have been unable to test the model at this time. However, we anticipate this will be completed in the near future.

Software Development. The development of software modules for the continuum-level electrochemical model is in progress. We also intend to offer them to the teams at ORNL, NETL and PNNL for pre-testing to determine their compatibility with existing failure analysis software, and we will make them available to the SECA industrial teams shortly thereafter. At this point, the project for the *steady-state* continuum-level electrochemical model for defect generation and

transport has been completed. Two languages were used, C++, because it is the industry standard, and PHP, because of its web-oriented features.

Conclusions

- A continuum-level electrochemical model has been developed that improves on preceding efforts by including a non-linear potential distribution and by including potential-dependent boundary conditions.
- The continuum-level electrochemical model has been extended to describe thermo-mechanical, thermochemical and transient stability in MIECs.
- Experimental results concur with the predictions of the continuum-level electrochemical model for electrical conductivity.
- Experimental results concur with the predictions of the continuum-level electrochemical model for thermo-mechanical properties.
- The steady-state version of the continuum-level electrochemical model has been written in C++ and PHP.

References

1. H. L. Tuller, Nonstoichiometric Oxides, ed. O. Sorensen (Academic, N. Y., 1981) ch. 6.

2. K. Duncan, Ph. D. Thesis, University of Florida (2001).

3. K. Eguchi, T. Setoguchi, T. Inoue and H. Arai, Solid State Ionics 52 (1992) 265.

4. J. Newman, Electrochemical Systems (Prentice-Hall, 1991).

5. E. Wachman and K. Duncan, Stable High Conductivity Bilayered Electrolytes for Low Temperature SOFCs, DOE Final Report, Contract No. DE-AC26-99FT40712, 2002.

6. I. Riess, J. Electrochem. Soc. 128 (1981) 2077.

7. M. Liu, J. Electrochem. Soc. 144 (1997) 1813.

8. S. Yuan and U. Pal, J. Electrochem. Soc. 143 (1996) 3214.

9. P. J. Gellings, H. J. A. Koopmans and A. J. Burggraaf, App. Catalysis 39 (1988) 1.

10. M. Barsoum, in Fundamentals of Ceramics (McGraw-Hill, 1977).

11. D-J. Kim, J. Amer. Ceram. Soc. 72 (1989) 1415.

12. M. Zacatea, L. Minervinia, D. Bradfielda, R. Grimes and K. Sickafus, Solid State Ionics 128 (2000) 243.

FY 2004 Publications/Presentations

1. "Determination of Electrochemical Performance and Thermo-Mechanical-Chemical Stability of SOFCs from Defect Modeling," US Department of Energy, Solid State Energy Conversion Alliance Workshop, September 30 - October 1, 2003, Albany, NY.

2. "Low-Temperature Solid Oxide Fuel Cells Based on Stable High Conductivity Bilayered Electrolytes," Fuel Cell Seminar, November 3-6, 2003, Miami, FL.

3 "Determination of Electrochemical Performance and Thermo-Mechanical-Chemical Stability of SOFCs from Defect Modeling," US Department of Energy, Solid State Energy Conversion Alliance Workshop, May 11-13, 2004, Boston, MA.

4 "Effect of Tertiary Phase Formation at the LSM/YSZ Interface on the Cathodic SOFC Reaction," 6th International Symposium on Electrochemical Impedance Spectroscopy, May 16-21, 2004, Cocoa Beach, FL.